NIST-GCR-94-647

FIRE GROWTH MODELS FOR MATERIALS

J. G. Quintiere and B. Rhodes
Department of Fire Protection Engineering
University of Maryland
College Park, MD 20742

Issued June 1994
January 1994

Sponsored by:
U.S. Department of Commerce
Ronald H. Brown, *Secretary*
Technology Administration
Mary L. Good, *Under Secretary for Technology*
National Institute of Standards and Technology
Arati Prabhakar, *Director*

Notice

This report was prepared for the Building and Fire Research Laboratory of the National Institute of Standards and Technology under grant number 60NANB2D1266. The statements and conclusions contained in this report are those of the authors and do not necessarily reflect the views of the National Institute of Standards and Technology or the Building and Fire Research Laboratory.

FIRE GROWTH MODELS FOR MATERIALS

James Quintiere and Brian Rhodes
Department of Fire Protection Engineering
University of Maryland
College Park, MD 20742

Report Date:
January, 1994

Final Report:
June 1992 - December 1993

Grant Number: 60NANB2D1266

ABSTRACT

Ignition and burning rate data have been developed for thick (25 mm.) black Polycast PMMA in a Cone Calorimeter heating assembly. The objective was to establish a testing protocol that would lead to the prediction of ignition and burning rate from Cone data. This has been done for a thermoplastic like PMMA. For black PMMA we measured ignition temperatures of 250 to 350 C and vaporization temperatures of approximately 325 to 380 C over irradiance levels of 15 to 60 kW/m^2. The incident flame heat flux, for irradiation levels of 0 to 75 kW/m^2, was found to be approximately 37 kW/m^2 for black PMMA. Its constancy has been shown due to the geometry of the Cone flame. Also, this flame can be shown to be nearly transparent for Cone irradiance (greater than 90 percent). The heat of gasification of the black PMMA used was found to be approximately 2.8 kJ/g; higher than other values reported for PMMA. This is believed to be due to differences in molecular structure or pigmentation effects and the types of PMMA tested. A burning rate model was demonstrated to yield good accuracy (greater than 80 percent) in comparison to measured transient values.

Keywords: burning rate, data, ignition, heat flux, model, PMMA

TABLE OF CONTENTS

	Page
List of Figures	xi
List of Symbols	xiii
Introduction	1
Approach	1
Experimental Apparatus and Measurements	3
Ignition	7
Burning Rate	11
Simulated Sample	12
Models	12
Preheating to Ignition	12
Burning Rate	20
Flame Radiation	23
Results	24
Ignition	25
Burning Rate	27
Conclusions	36
Acknowledgement	37
References	38

LIST OF FIGURES

Number		Page
1	Schematic layout of burning rate apparatus	4
2	Photograph of burning rate apparatus	5
3	Photograph of flaming PMMA sample	6
4	Surface temperature of black PMMA as a function of time with a 19 kW/m^2 external heat flux	8
5	Ignition and vaporization temperature of black PMMA as a function of external heat flux	9
6	Calculated and measured ignition time of black PMMA as a function of external heat flux	10
7	Transient mass loss rate of black PMMA with a 25 kW/m^2 external heat flux	13
8	Net surface heat flux measured by sensor of black PMMA with a 25 kW/m^2 external heat flux	14
9	Non-flaming transient mass loss rate of black PMMA with a 21 kW/m^2 external heat flux	15
10	Non-flaming net surface heat flux measured by sensor of black PMMA with a 25 kW/m^2 external heat flux	16
11	Steady state heat flux measured by sensor of methane gas burner with a 50 kW/m^2 external heat flux	17
12	Ignition data for black PMMA	26
13	Steady state mass loss rate as a function of external heat flux for flaming and non-flaming PMMA	29
14	Calculated and measured flame plus external heat flux as a function of external heat flux for black PMMA	30
15	Calculated transient mass loss rates of black PMMA with a 25 kW/m^2 external heat flux	32
16	Calculated transient mass loss rates of black PMMA with a 50 kW/m^2 external heat flux	33

Number Page

17 Calculated transient mass loss rates of black PMMA with a 75 kW/m^2 external heat flux 34

18 Calculated transient mass loss rates of black PMMA using calculated and literature material property values 35

LIST OF SYMBOLS

c - specific heat

E/R - material constant (Eq. 4)

h_c - convective heat transfer coefficient

k - thermal conductivity

l - beam length

L - heat of gasification

m - mass

Q - power output

q - heat flow

r - stoichiometric oxygen to fuel mass ratio

T - temperature

t - time

y - space coordinate

$Y_{ox,\infty}$ - ambient oxygen mass fraction

α - thermal diffusivity

δ - thermal penetration depth

ΔH_v - heat of vaporization

ΔH_c - heat of combustion

ε - emissivity

κ - absorption-emission coefficient

ρ - density

σ - Stefan Boltzmann constant

ξ - variable (Eq. 20)

χ - heat fraction

Subscript

c - convective

cr - critical

e - external

fl - flame

f,c - flame convection

f,r - flame radiation

g - gas

ig - ignition

o - initial, ambient

m - mean

r - radiative

s - steady

sens - sensor

v - vaporization

w - water

Superscripts

$(\dot{})$ - per unit time

$(\,)''$ - per unit area

FIRE GROWTH MODELS FOR MATERIALS

Introduction

The objective of this research is to develop transient burning rate models from data derived from the Cone Calorimeter [1]. It is sought to do this in a way that is consistent with the testing of materials by standard practices. The models will be dependent on the class of materials; namely, thermoplastic, charring, dripping, and laminated. Initially, thermoplastics, thick enough to not be affected by their substrate and large enough to be considered approximately one-dimensional in behavior, will be considered. Black PMMA (25 mm thick) has been chosen as representative of this class, and was used in this initial study.

Ultimately, these burning rate models will be incorporated into fire growth simulations [e.g. 2, 3, 4, 5] to give more accurate predictions of hazard. However, the first step is to succeed, for at least thick thermoplastics and charring materials, in developing a viable strategy for using the Cone data for transient burning rate predictions.

It is recognized that several studies are seeking to address this objective with modeling strategies that differ from that to be presented [6, 7, 8]. We believe our approach is the simplest in form and the most reasonable to practically implement. But we do not sacrifice phenomenological significance. The model is based on the integral formulation outlined by Quintiere [9], and implemented by Quintiere and Iqbal [10] for non-flaming pyrolysis of a thermoplastic. Moreover, a very similar and successfully applied pyrolysis model for PMMA has been presented by Agrawal and Atreya [11]. The details will follow.

Approach

The Cone Calorimeter is a widely used device to measure the mass loss ($\dot{m}''$) and energy release ($\dot{Q}''$) rates per unit area under a specified external radiative heat flux. The ratio of these two quantities gives the instantaneous heat of combustion (ΔH_c) relative to the gaseous fuel produced during flaming combustion. Generally, during flaming combustion, it has been shown that this heat of combustion is approximately constant for the material. In the least, it can be measured, and

is not expected to be scale dependent, i.e. change as a larger area of fuel is burned. Also, except for multi-dimensional effects involving seams, joints, edges, etc., the thermal and chemical properties of the decomposing material would also be independent of scale. In contrast, the heat flux $(\dot{q}'')$ to the material's surface would depend on scale and on test conditions in the Cone Calorimeter. Hence, it follows that under these one-dimensional burning conditions,

$$\dot{m}'' = f(q'', \text{thermo-chemical properties}) \qquad (1)$$

and,

$$\dot{Q}'' = \dot{m}'' \Delta H_c. \qquad (2)$$

Equation (1) symbolically represents a model involving the surface heat flux and the needed properties. We will examine a specific model for a vaporizing thermoplastic-like material. Experimentally we shall consider black PMMA.

A cone heater apparatus was used with a continuous mass loss recording. Both the processes of ignition and burning rate were examined between 0 and 75 kW/m^2 irradiance. In order to assess the total heat flux required by Eq. (1), both the external radiant heat flux and the flame heat flux were monitored. This was done with a small diameter (3 mm) water cooled thermopile type heat flux gage. Measurements were conducted until steady burning. These measurements gave two methods for determining the incident flame heat flux (convection plus radiation). The first was from the gage directly; the second from steady burning in which Eq. (1) reverts to,

$$\dot{m}'' = \frac{\dot{q}''}{L} \qquad (3)$$

where $\dot{q}''$ is the net surface heat flux,

and L is the effective heat of gasification.

The results of these measurements and analyses will be discussed.

In order to assess the effects of flame absorption on the external radiant flux imposed from

the cone heater, a simulated sample was employed. This consisted of a glass beaded burner matrix with a center slot for the heat flux meter. Methane was supplied at fixed rates in a standard cone mounting. Other gases, with different radiative absorbing characteristics will be used in the future.

The data taken from these experiments were examined in conjunction with ignition and burning rate models designed to elucidate the needed thermochemical properties. We concede that these properties will be model dependent, but not devoid of physical significance nor in extreme conflict with their more precisely derived counterparts. However, we believe the simplicity of these models will have potential utility.

The experimental and modeling details will be reviewed and their results presented. A recommended testing protocol for thermoplastics will be presented as a result. Its usefulness will be assessed in the future by examining its applicability to other thermoplastics.

Experimental Apparatus and Measurements

Figure 1 shows the schematic layout of the burning rate apparatus. A photograph of the system is shown in Figure 2. The sample is placed on a standard cone metal holder on a bed of Kaowool. The black PMMA (100 mm x 100 mm x 25 mm thick) is constrained at the side edges by bonded cardboard. This enables more uniform one-dimensional burning and eliminates side burning. The sample has a center hole that allows freedom of movement of the heat flux gage during continuous mass loss measurement of the sample. The heat flux gage was cooled with water at 65 degrees Celsius to reduce the prospect of condensation. However, condensation and re-evaporation of PMMA monomer still occurred. This gave positive and negative respective responses to the heat flux gage, independent of the incident heat flux. Also, it was found that insulating the gage on its sides minimized extraneous results. In short, this measurement of heat flux was not easily accomplished. As a result, we only included the results when these effects were minimized the most.

Figure 3 shows a burning sample which illustrates the typical elongated column flame that protrudes through the top of the cone heater. The flame length to effective diameter (sample face) ratio is of the order of 4. This is significant in estimating the mean beam length for typical flames under the cone heater.

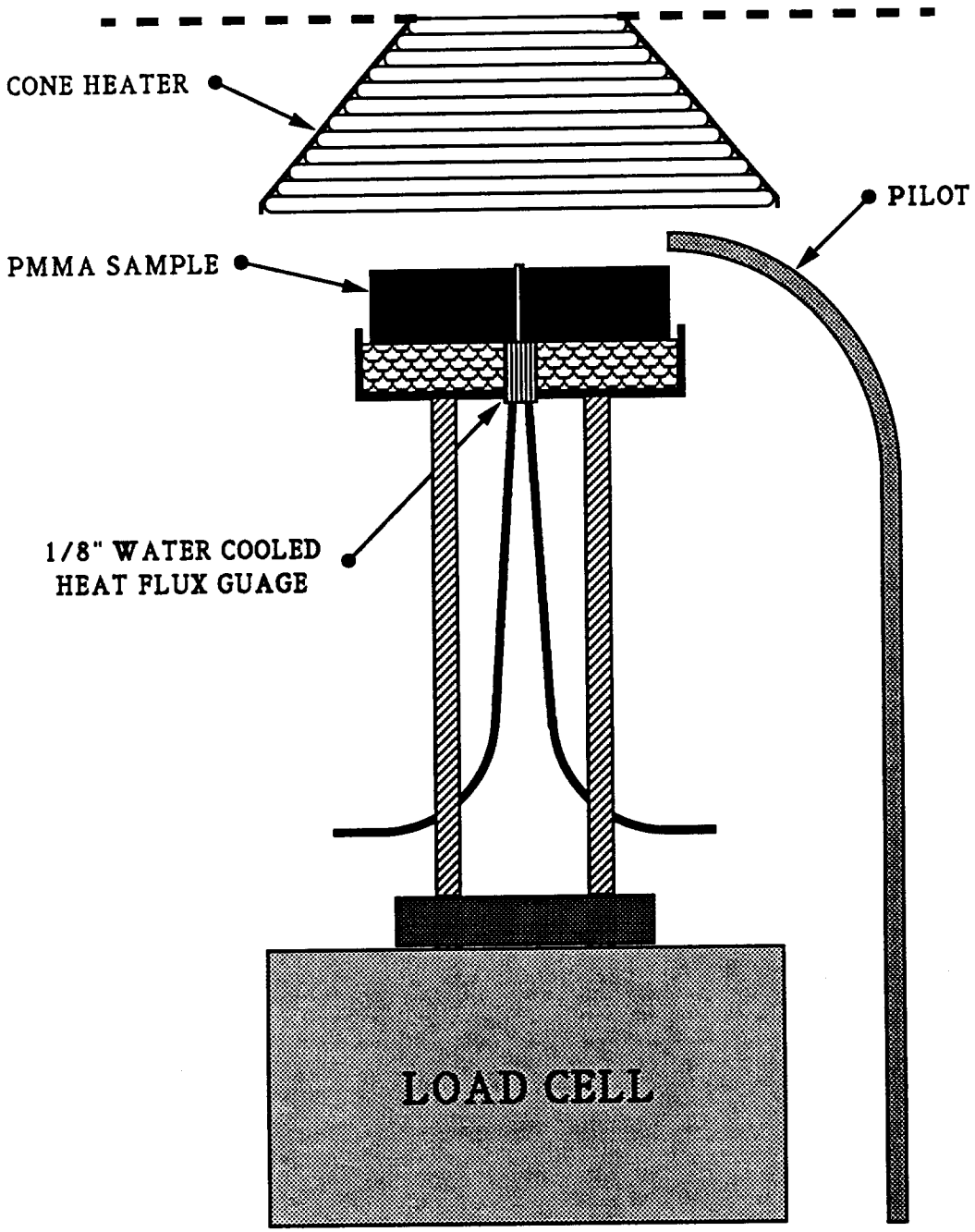

Figure 1. Schematic layout of burning rate apparatus

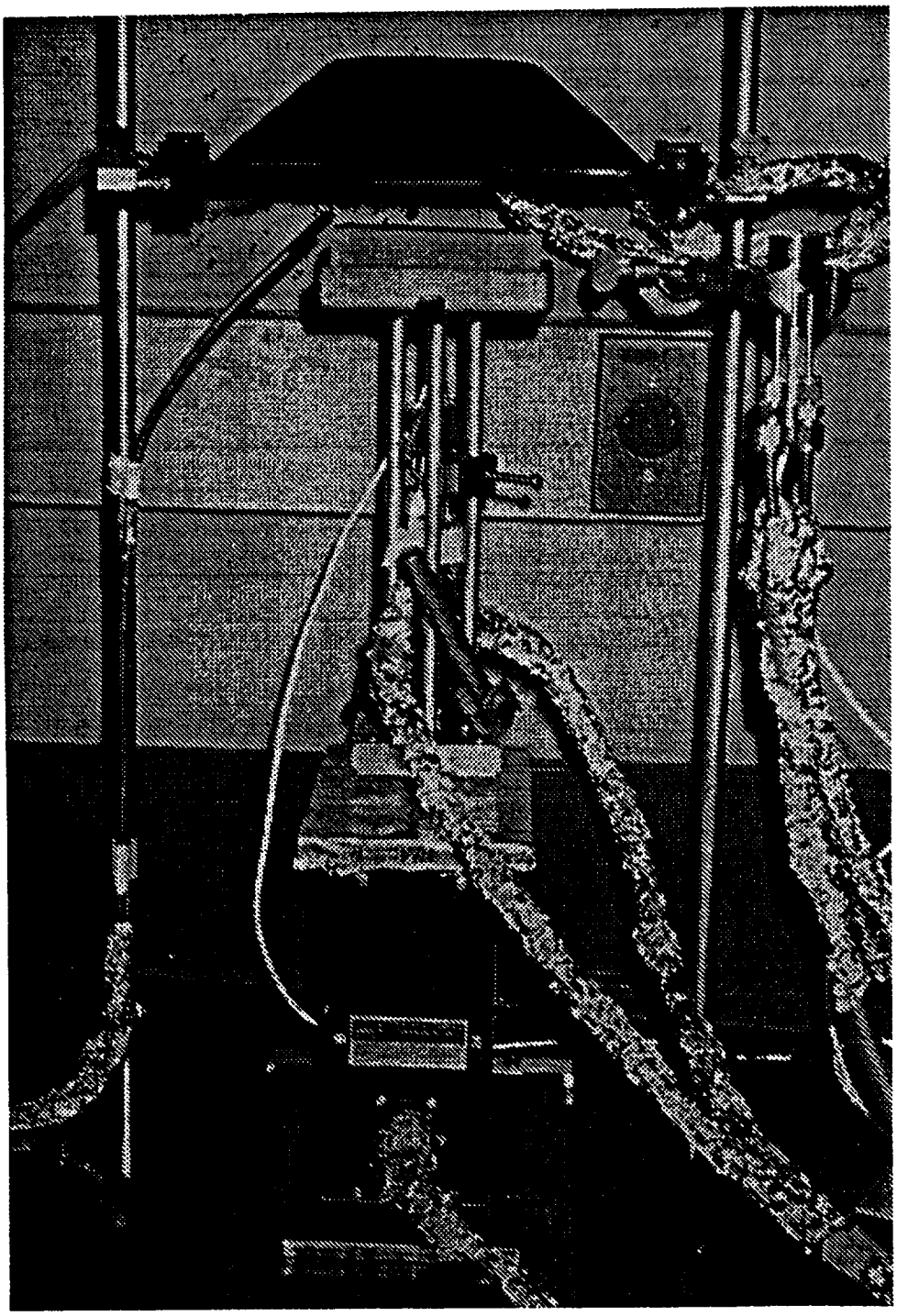

Figure 2. Experimental burning rate apparatus

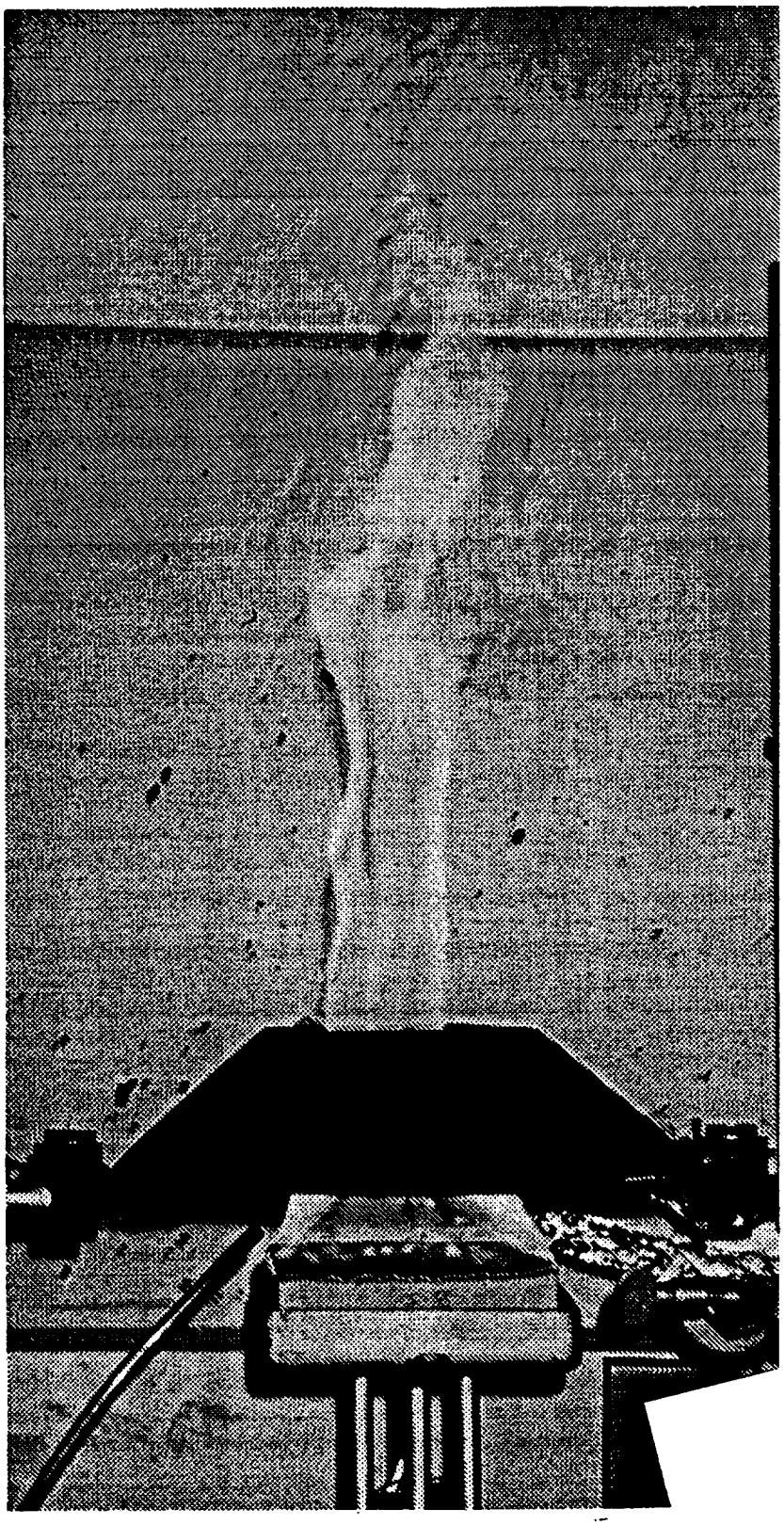

Figure 3. Flaming PMMA sample

Ignition

The experimental procedure consisted of irradiating the sample at a fixed external flux. A non-contacting pilot flame at the edge triggered ignition. In some cases, a fine wire Type K thermocouple (.005 inches diameter) was used to measure the surface temperature up to the onset of burning. It was mounted on the PMMA by heating the thermocouple wire such that it recessed into the surface. A typical result is shown in Figure 4 for an irradiance of 19 kW/m^2. Ignition is indicated by the sudden step-like increase and the subsequent plateau which indicates the affect of the added flame heat flux. We define the temperature at the onset of the "jump" as the ignition temperature (T_{ig}) and at the onset of the plateau as the vaporization temperature (T_v). The latter is related to the mass loss rate since pyrolysis is more appropriately related to temperature e.g. in Arrhenius form given by Vovelle at al. [12],

$$\dot{m}'' \sim e^{-E/RT} \qquad (4)$$

where E/R is a material constant. We shall alternatively adopt a model which uses a fixed vaporization temperature which is valid for large burning rates. Figure 5 shows our results for T_{ig} and T_v expressed as functions of external incident radiant heat flux. These temperatures increase with heat flux as a result of the behavior expressed by Eq. (4). Thompson and Drysdale [13] make a further distinction between flashpoint temperature (at flashing) and firepoint temperature (at sustained ignition) for T_{ig}. They report for a horizontal orientation of PMMA a flashpoint of approximately 265 degrees Celsius and a fire point of 300 degrees Celsius for external heat fluxes of 13 to 35 kW/m^2. These are consistent with our ignition temperatures in the same range of heat flux, but we did not make this fine of a discrimination.

Kashiwagi and Omori [14] investigated piloted ignition of two different class PMMA samples (75 mm x 75 mm x 13 mm thick): one high molecular weight (MW), "thermally stable"; and the other a low MW, "thermally unstable". The surface temperatures at piloted ignition ranged from 320 to 340 degrees Celsius for the high MW PMMA, and 260 to 270 degrees Celsius for the low MW samples irradiated between 10 to 20 kW/m^2 respectively. The low MW results appear to be consistent with Thompson and Drysdale [13] and our results.

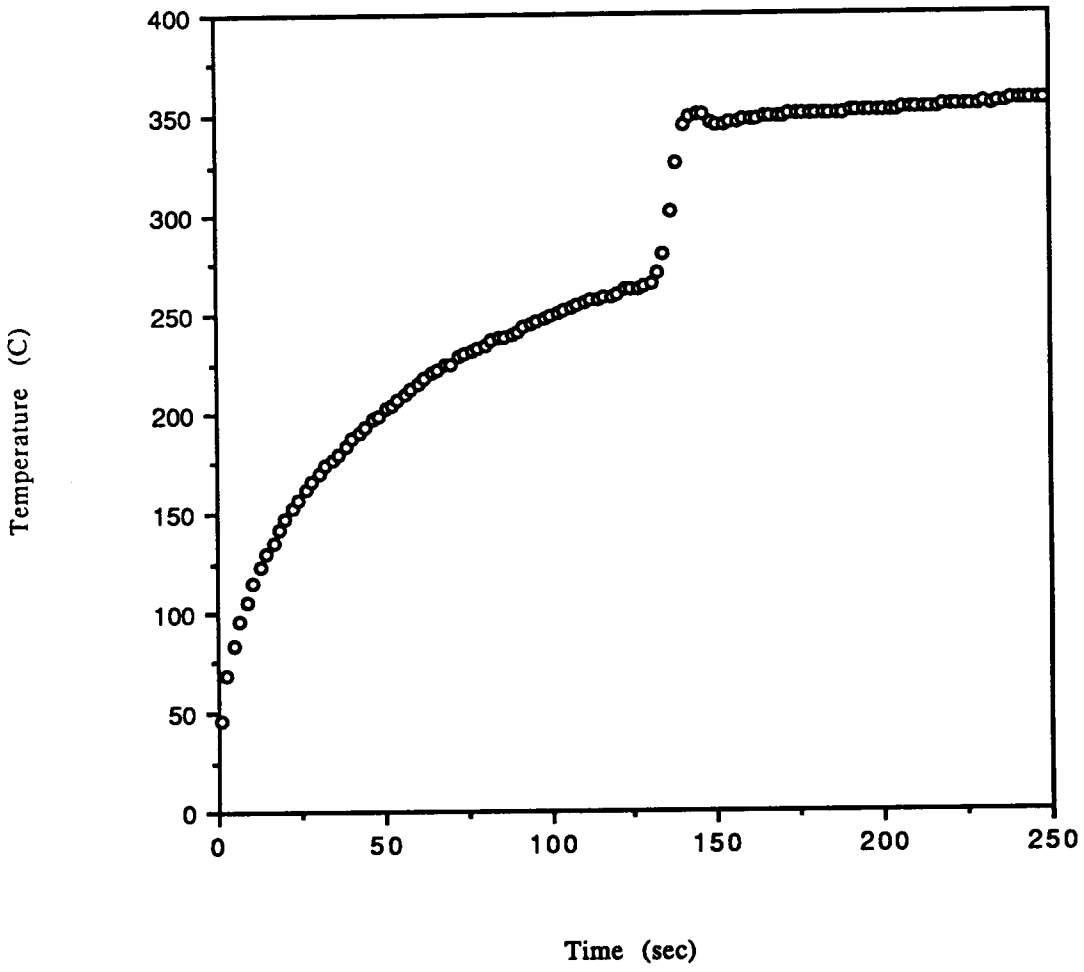

Figure 4. Surface temperature of black PMMA as a function of time with a 19 kW/m^2 external heat flux

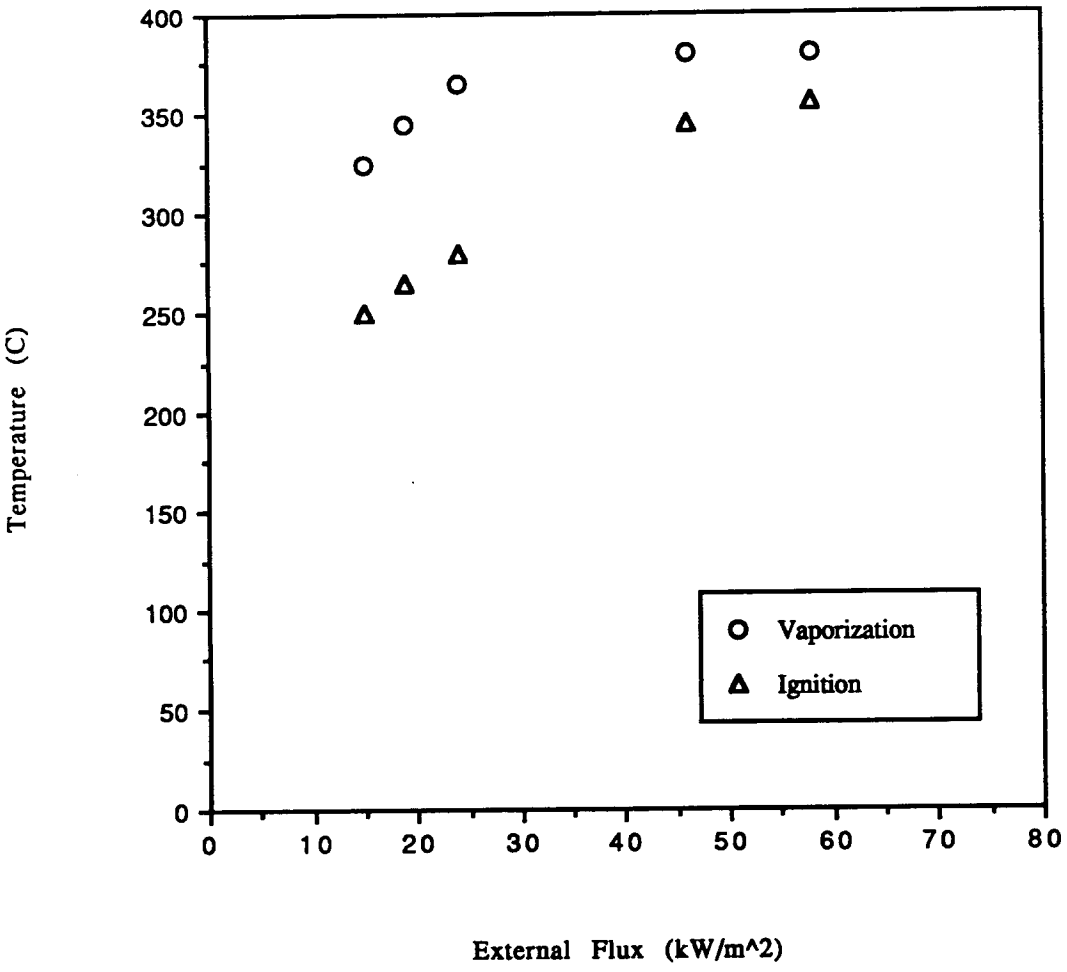

Figure 5. Ignition and vaporization temperature of black PMMA as a function of external heat flux

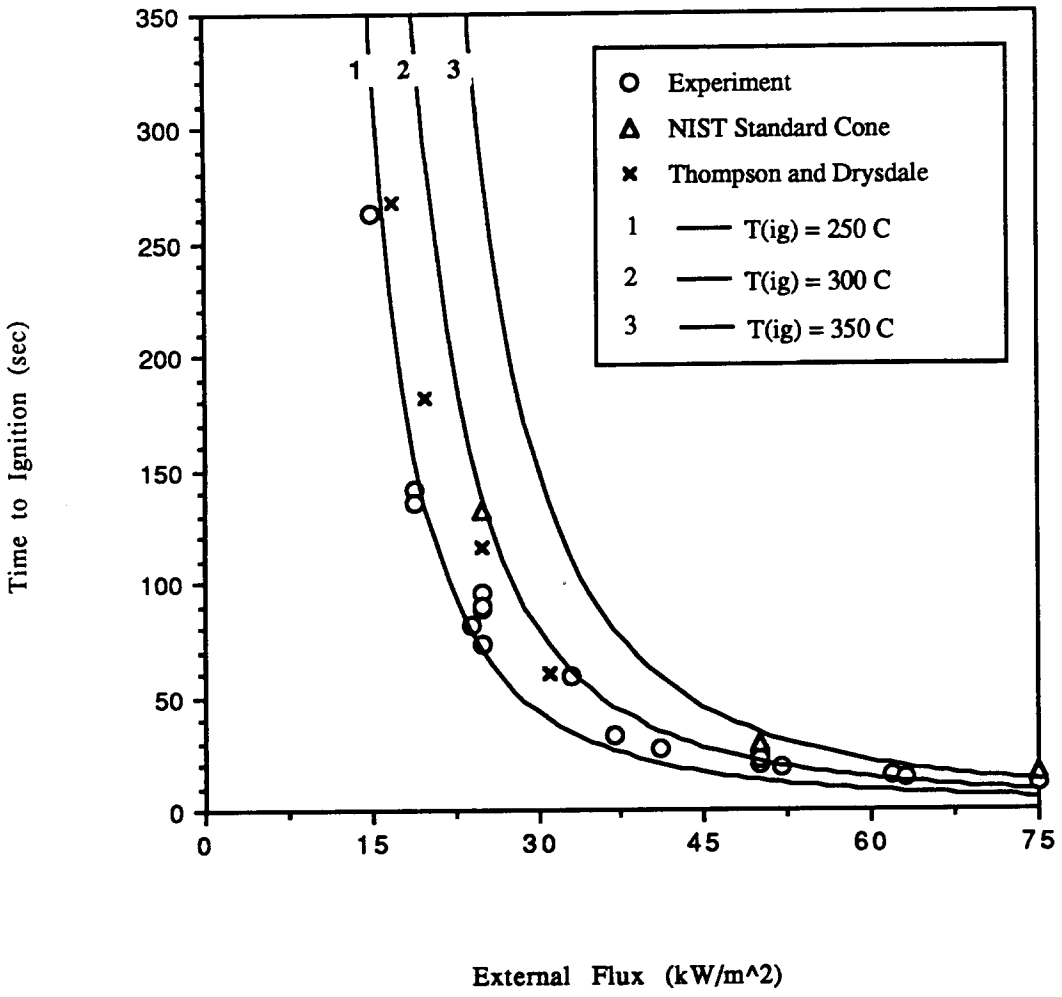

Figure 6. Calculated and measured ignition time of black PMMA as a function of external heat flux

Time to ignite as a function of external radiant flux is given in Figure 6. The standard NIST Cone electric spark piloted apparatus gave longer ignition times than our flame piloted system. The location of the pilot is probably the reason. The results by Thompson and Drysdale [13] are just slightly higher than ours. Other results by Mikkola and Wickman [15] for black PMMA are consistent. The ignition times of Kashiwagi and Omori [14] appear to bracket our results with the low MW agreeing more at 20 kW/m^2 and the high MW at 10 kW/m^2. They measured an ignition time of 900 seconds for the high MW PMMA at approximately 9 kW/m^2. We have not measured, nor have found in the literature, a measured minimum heat flux for piloted ignition of PMMA.

Burning Rate

Figures 7 and 8 depict the mass loss rate and net surface heat flux measured by the sensor, respectively, for an external radiant flux of 25 kW/m^2. These are representative results taken over 0 to 75 kW/m^2. The increase in heat flux initially before ignition is due to convective heating. At ignition (~ 90 sec), there is a sharp rise in the burning rate and in the heat flux. The initial flame heat flux appears to be approximately 22 kW/m^2. We will later conclude that this is low, probably due to the deposition of condensable monomer on the heat flux sensor. Condensation can add heat to the sensor, but the initial deposition may shield it. Subsequent evaporation of the monomer could also reduce the heat flux. These processes undoubtedly affected the accuracy of this measurement. The subsequent "jump" at about 240 seconds in Figure 8 is indicative of the anomalies experienced in this measurement. Surprisingly, the heat flux gage was very robust, and despite deposition, it was within 10 percent of calibration following each test under external radiant heat transfer.

Figures 9 and 10 depict mass loss and surface heat flux to the sensor, respectively, for nonflaming conditions at an external radiant heating of 21 kW/m^2. The five point running differentiation of the mass loss signal does not lead to a smooth mass loss curve at this low range. However, the nominal value of 5 g/m^2-s at equilibrium is consistent with expected results [14]. This radiant heat flux implies a maximum convective flux loss of 4 kW/m^2 (25 - 21) from Figure 10 due to the sample heating. For a vaporization temperature of 365 degrees Celsius (Fig. 5),

assumed to be the local gas temperature, exposed to the heat flux gage at 65 degrees Celsius, yields a convective heat flux coefficient of approximately 13 W/m^2-K which is consistent with natural convection correlations. No extensive study was done of the nonflaming case.

Simulated Sample

A glass bead burner equal to the size of a PMMA sample was used to simulate a burning sample. Methane was used as the fuel and the center surface heat flux was measured with the heat flux gage. No fouling problems were present for these tests. Figure 11 shows the steady state sensor heat flux measurements with an external cone exposure of of 50 kW/m^2. The results tend to show a constant flame heat flux above the external radiant flux. This is approximately 27 kW/m^2 over a range of energy release rates per unit area of 200 to 600 kW/m^2 consistent with the PMMA energy release rates. Thus, despite the increased flame heights, due to increased burning rates, the flame heat flux is approximately constant. We will explain this later.

Models

The models used in the analyses are based on the presentation of Quintiere and Iqbal [10]. These use an integral model for one dimensional unsteady conduction and surface vaporization at a fixed temperature. The models are outlined below:

Preheating to Ignition

The governing equation is,

$$\frac{\partial T}{\partial t} = \alpha \frac{\partial^2 T}{\partial y^2} \qquad (5)$$

where, T is temperature,

t is time,

y is distance measured from the surface,

α is the thermal diffusivity, $\frac{k}{\rho c}$,

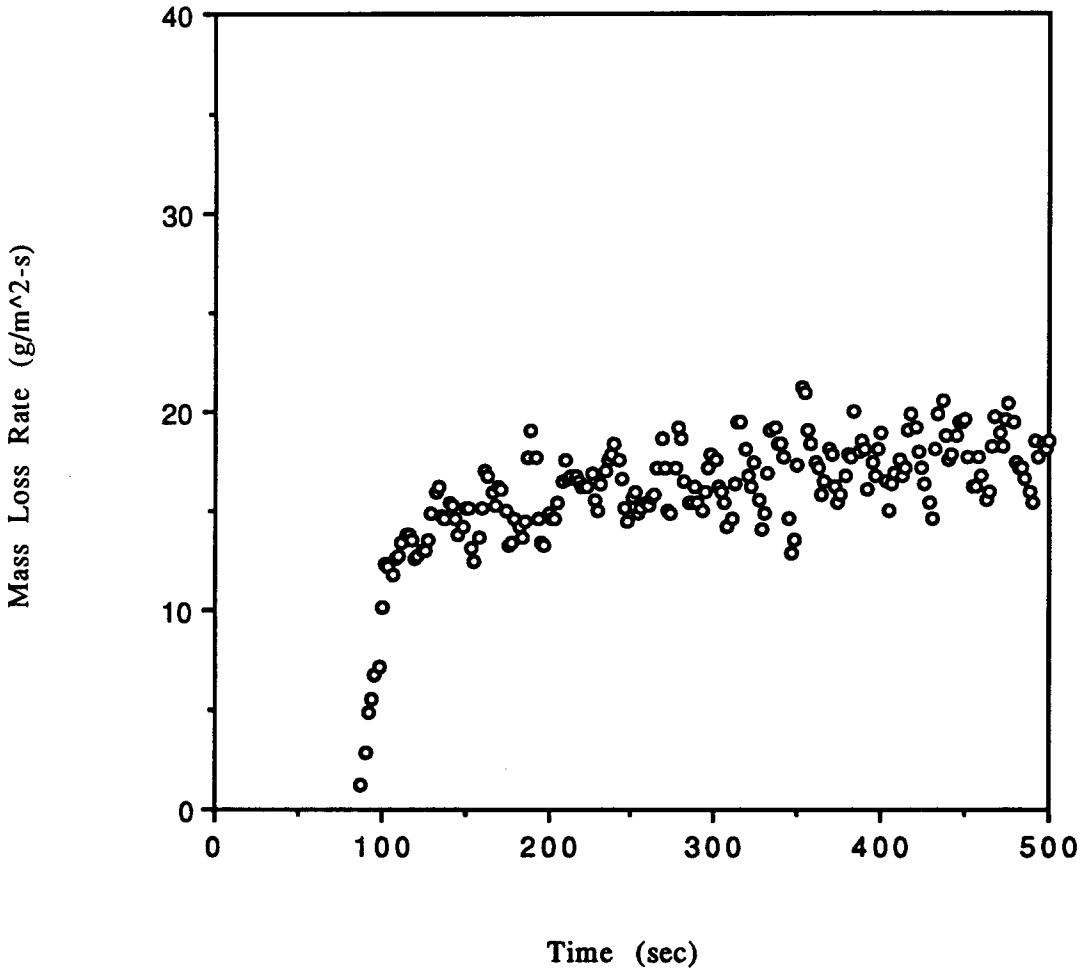

Figure 7. Transient mass loss rate of black PMMA with a 25 kW/m^2 external heat flux

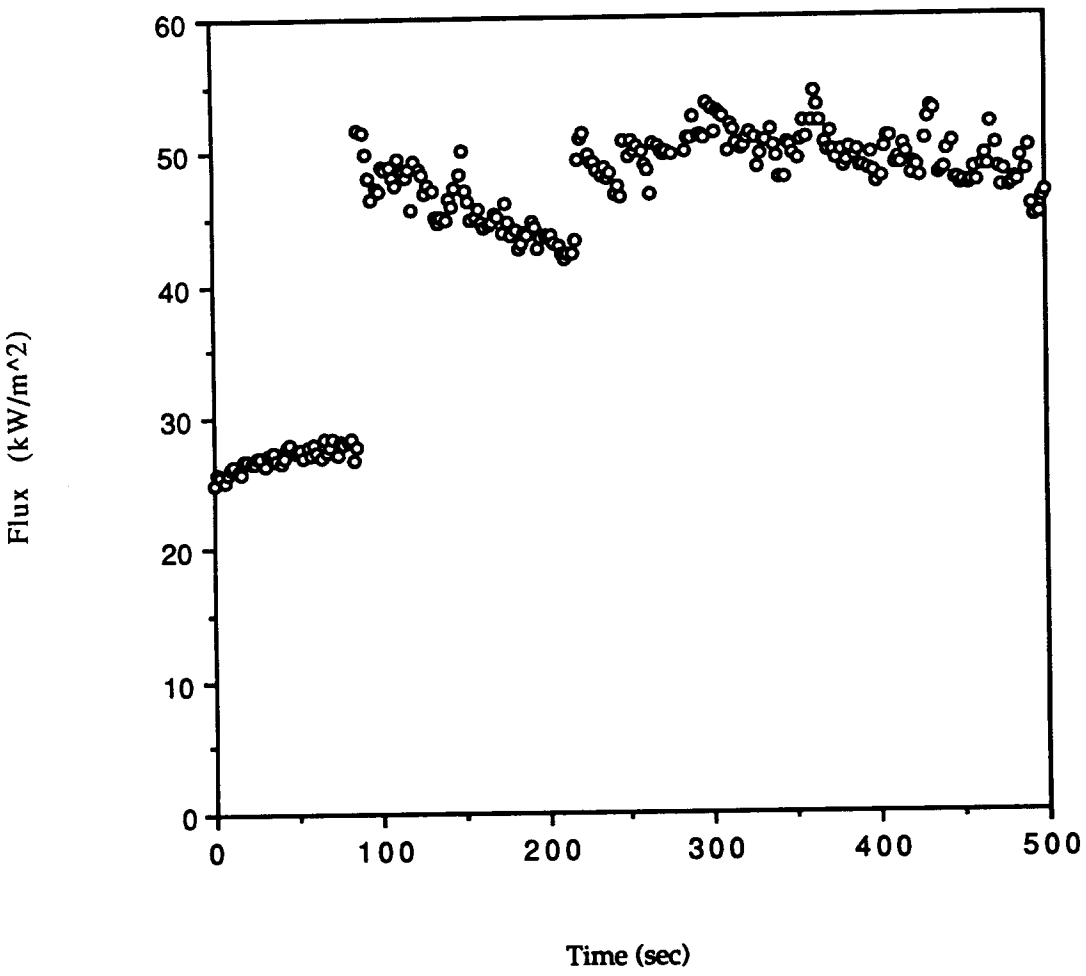

Figure 8. Net surface heat flux measured by sensor of black PMMA with a 25 kW/m^2 external heat flux

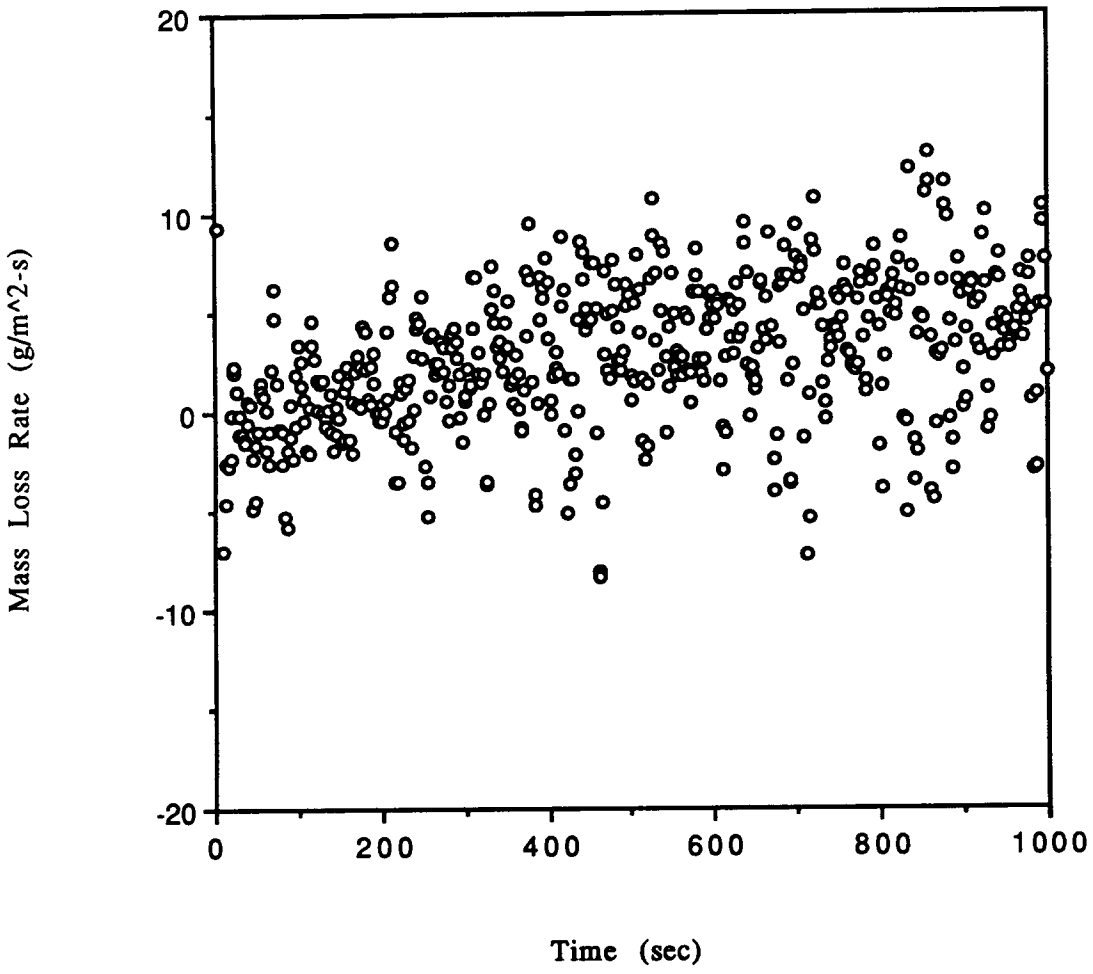

Figure 9. Non-flaming transient mass loss rate of black PMMA with a 21 kW/m^2 external heat flux

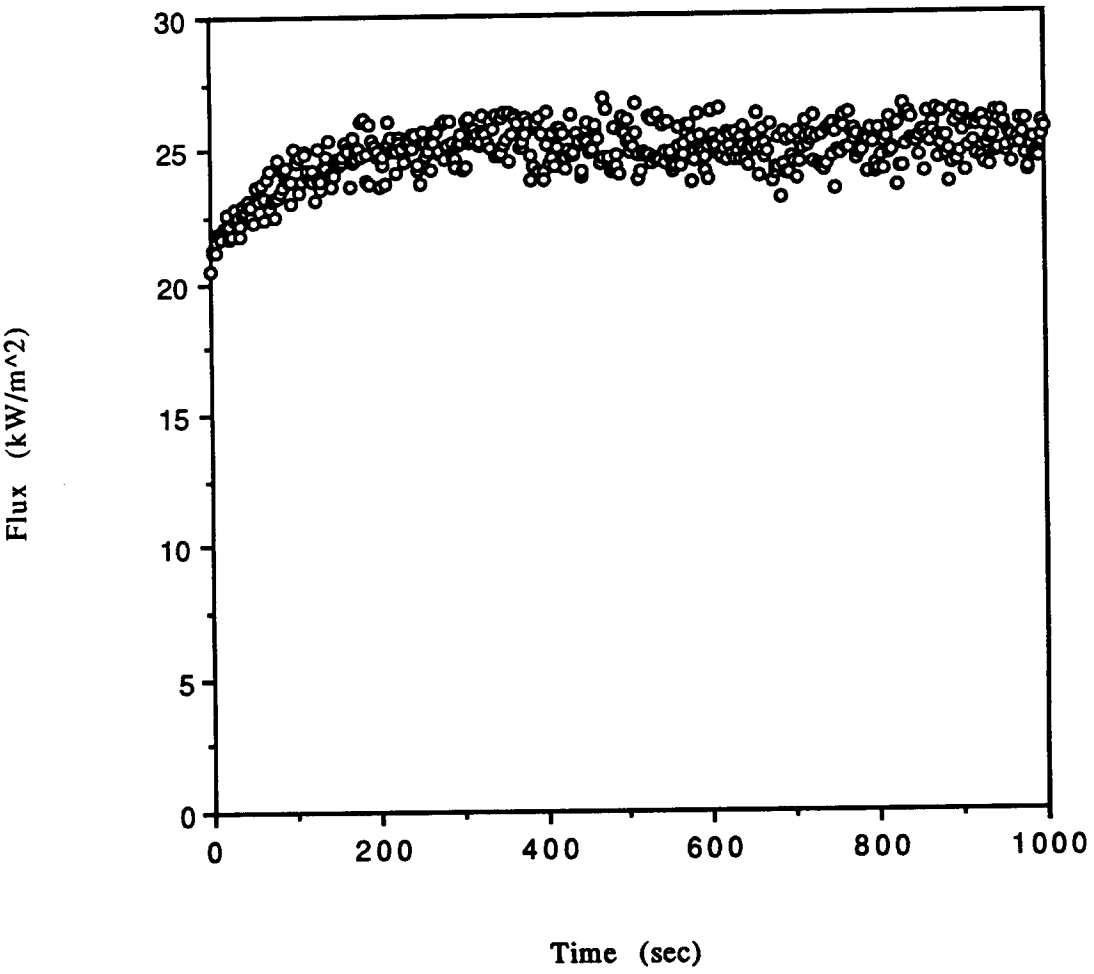

Figure 10. Non-flaming net surface heat flux measured by sensor of black PMMA with a 25 kW/m^2 external heat flux

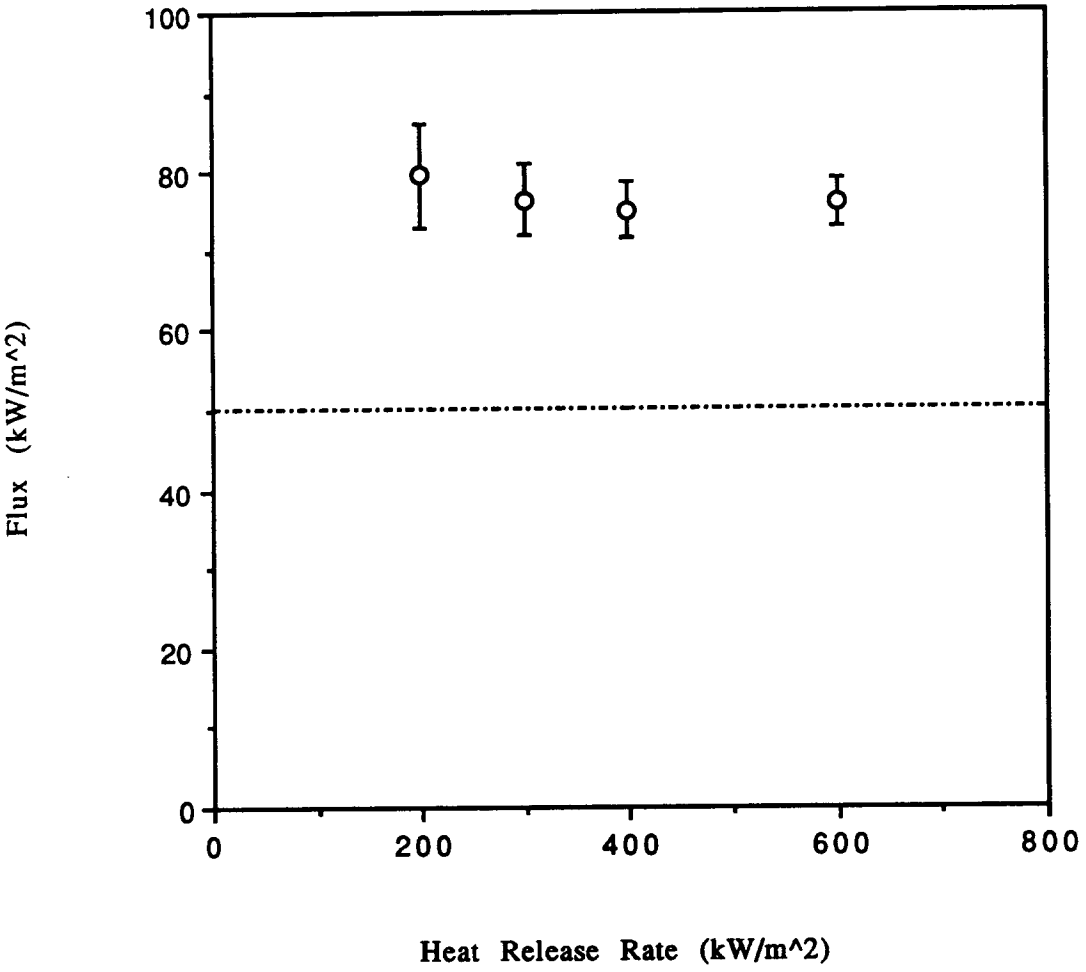

Figure 11. Steady state heat flux measured by sensor of methane gas burner with a 50 kW/m^2 external heat flux

k is the thermal conductivity,

ρ is the density,

and c is the specific heat.

Properties are assumed constant. The equation is integrated over $0 \le y \le \delta$ where at $y = \delta$,

$$T = T_o, \qquad (6a)$$

and,

$$\frac{\partial T}{\partial y} = 0. \qquad (6b)$$

At $y = 0$,

$$- k \frac{\partial T}{\partial y} = \dot{q}'' \equiv \varepsilon \, \dot{q}''_{ext} - h_c (T - T_o) - \varepsilon \, \sigma \, T^4 \qquad (7)$$

where, $\dot{q}''$ is the net surface heat flux,

ε is the surface emissivity and absorptivity,

h_c is the convective heat transfer coefficient,

$\dot{q}''_{ext}$ is the external incident radiative heat flux,

and σ is the Stefan-Boltzmann constant.

A quadratic profile is assumed such that the boundary conditions are satisfied:

$$T - T_o = \frac{\dot{q}'' \delta}{2 k} \left(1 - \frac{y}{\delta}\right)^2 \qquad (8)$$

It can be shown that,

$$\frac{d}{dt}\left(\dot{q}'' \delta\right) = 6 \alpha \dot{q}'' \qquad (9)$$

If we assume $\dot{q}''$ is constant, which is a good assumption for $\dot{q}''_{ext}$ high enough, then,

$$\delta \cong \sqrt{6 \alpha t}. \qquad (10)$$

It has been shown by Abu-Zaid and Atreya [16] that a more complete solution to the above problem yields:

$$\delta = \sqrt{\frac{12 \alpha t}{e_4}} \qquad (11)$$

where e_4 was shown to vary between 1.6 at 15 kW/m^2 to 1.9 at 50 kW/m^2. If we take the asymptote as 2.0 we obtain the approximate result of Eq. (10). In terms of the fire modeling we are attempting, we will sacrifice this accuracy since the solution is approximate anyway. But at very low heat fluxes, the error introduced will be greatest.

Substituting into Eq. (8) at y = 0 gives:

$$T_{ig} - T_o = \frac{\dot{q}'' \delta}{2 k} = \frac{\dot{q}''}{2 k} \sqrt{6 \alpha t_{ig}} \qquad (12)$$

or,

$$t_{ig} = \frac{2}{3} (k \rho c) \frac{(T_{ig} - T_o)^2}{(\dot{q}'')^2}. \qquad (13)$$

Note that this algorithm also gives a means for computing the surface temperature over time. This is done implicitly by selecting T_s, computing the corresponding net heat flux, and using Eq. (13) to

find the time. Moreover, this result allows a computation of the critical flux, $\dot{q}''_{cr}$, for ignition by extrapolating ignition data for $(t_{ig})^{-1}$ to zero. At this intercept,

$$\dot{q}''_{ext} = \frac{1}{\varepsilon}\left[h_c\,(T_{ig} - T_o) + \varepsilon\,\sigma\,T_{ig}^4\right] \equiv \dot{q}''_{cr}. \qquad (14)$$

From Eq. (7) and (13) the critical flux is found. Eq. (13) is in contrast to the analytical fit to the exact solution offered by Janssens [17]:

$$\dot{q}''_{ext} = \dot{q}''_{cr}\left[1 + 0.73\left(\frac{k\,\rho\,c}{h_c^2\,t_{ig}}\right)^{0.547}\right]. \qquad (15)$$

Burning Rate

The governing equation for the burning rate problem follows from Eq. (5) which governs conduction below the moving vaporizing surface at a fixed vaporization temperature, T_v. Hence at $y = 0$,

$$T = T_v \qquad (16)$$

and also,

$$-k\frac{\partial T}{\partial y} = \dot{q}'' - \dot{m}''\,\Delta H_v \qquad (17)$$

where, $\dot{m}''$ is the mass loss rate per unit area,

ΔH_v is the heat of vaporization,

and $\dot{q}''$ is the net surface heat flux.

$$\dot{q}'' = \varepsilon \dot{q}''_{ext} + \dot{q}''_{fl} - \varepsilon \sigma T_v^4 \qquad (18)$$

where $\dot{q}''_{fl}$ is the flame heat flux given as:

$$\dot{q}''_{fl} = \varepsilon \dot{q}''_{fl,r} + \dot{q}''_{fl,c} \,. \qquad (19)$$

The flame incident radiant heat flux is $\dot{q}''_{fl,r}$ and the convective flux, from a stagnation film flame model [9], can be shown as,

$$\dot{q}''_{fl,c} = \frac{h_c}{c_g}\left(\frac{\xi}{e^{\xi} - 1}\right)\left[Y_{ox,\infty}(1 - \chi_r)\frac{\Delta H_c}{r} - c_g (T_v - T_o)\right] \qquad (20)$$

where, $\xi = \dfrac{\dot{m}'' c_g}{h_c}$,

$\left(\dfrac{\xi}{e^{\xi} - 1}\right)$ is the mass transfer "blocking factor" that is one for $\dot{m}'' \rightarrow 0$,

$Y_{ox,\infty}$ is the ambient mass fraction of oxygen,

χ_r is the flame radiative fraction,

ΔH_c is the heat of combustion,

r is the stoichiometric fuel to oxygen mass ratio,

and c_g is the gas phase specific heat at constant pressure.

Alternatively, this might be expressed as,

$$\dot{q}''_{fl,c} = h_c \left(\frac{\xi}{e^{\xi} - 1} \right) (T_{fl} - T_v) \qquad (21)$$

where T_{fl} is an effective flame temperature.

Note that $\dot{q}''$ in Eq. (18) is different from that defined in Eq. (7).

Assuming a quadratic profile,

$$\frac{T - T_o}{T_v - T_o} = \left(1 - \frac{y}{\delta} \right)^2 \qquad (22)$$

which satisfies Eqns. (6) and (16). Substituting this profile in Eq. (17) provides,

$$\dot{m}'' \Delta H_v = \dot{q}'' - \frac{2k}{\delta} (T_v - T_o) \qquad (23)$$

where the last term is the conduction heat loss into the solid. Integration of Eq. (5) over y as before and substituting Eq. (22) yields,

$$\frac{1}{3} \frac{d\delta}{dt} + \frac{\dot{m}''}{\rho} = \frac{2\alpha}{\delta} \qquad (24)$$

where at ignition $T = T_v$ and $\delta = \sqrt{6 \alpha t_{ig}} = \delta_{ig}$.

If we ignore the dependence of the burning rate on the blocking factor, or if we assume the total flame heat flux is constant, Eq. (24) may be solved exactly. It can be shown that,

$$t - t_{ig} = \frac{\delta_s^2}{6\alpha} \frac{\Delta H_v}{L} \left[\frac{\delta_{ig} - \delta}{\delta_s} - \ln \left(\frac{\delta_s - \delta}{\delta_s - \delta_{ig}} \right) \right] \qquad (25)$$

where $\delta_s = \frac{2\,k}{c}\frac{L}{\dot{q}''}$, the steady value (26)

and $L = \Delta H_v + c\,(T_v - T_o)$, the heat of gasification. (27)

It follows that the steady state mass flux is given as,

$$\dot{m}_s'' = \frac{\dot{q}''}{L}. \qquad (28)$$

Note, in addition to the flame heat flux, the properties required to obtain a solution are ε, ρ, c, k, T_v, (or T_{ig}), and ΔH_v (or L). These must be derivable in a convenient way consistant with the burning rate and ignition models.

Flame Radiation

The emissivity of a flame can be represented as,

$$\varepsilon_{fl} = 1 - e^{-\kappa l_m} \qquad (29)$$

where, κ is the absorption coefficient,

and l_m is the mean beam length.

According to Orloff and deRis [18], κ and l_m can be computed from an algorithm for pool fires. By applying their algorithm, it was found than l_m/R (where R is the radius of the pool fire) is asymptotic at 1.3 for our PMMA cone assembly. Here we take 2R = 10 cm., the sample side dimension. If we consider a homogeneous grey gas cylindrical flame, $l_m = 0.65(2R)$ for a flame height greater than 4R [19]. Their prescription gives $\kappa = 1.4\ m^{-1}$ which compares to $1.3\ m^{-1}$ by measurement [20]. Also, Brosmer and Tien [21] consider $\kappa = 1.0\ m^{-1}$ for the PMMA fuel layer near the surface. An effective radiative flame temperature is reported as 1400 K [20]. This gives a flame emissivity of approximately 0.09 for the cone PMMA assembly. It also indicates that this

flame is very transparent (> 91%), and hence we can expect most of the Cone heat radiation to penetrate the flame and reach the surface. A cooler fuel layer would have a comparable effect on the PMMA flame. Moreover, for flame heights greater than 20 cm., the PMMA flame emissivity is approximately constant at 0.09.

The incident flame radiative heat flux is,

$$\dot{q}''_{fl,r} = \varepsilon_{fl} \sigma T_{fl}^4 \qquad (30)$$

For $T_f = 1400$ K, we estimate 20 kW/m^2. The convective heat flux (assuming a blocking factor of 1) can also be estimated by Eq. (20) considering,

$h_c = 10$ W/m^2·K $\qquad$ $\Delta H_c/r = 13$ kJ/g

$c_g = 1.0$ J/g·K $\qquad$ $\chi_r = 0.4$

$Y_{ox,\infty} = 0.233$

we find a maximum $\dot{q}''_{fl,c} = 15$ kW/m^2. Realizing $\varepsilon \approx 1$, this gives 35 kW/m^2 for $\dot{q}''_{fl}$.

This will be seen as fortuitously close to our experimental value, and must be viewed in that manner. But the constancy of the flame radiation heat flux for samples burning in the Cone Calorimeter is justified, and most materials are likely to have very transparent flames with respect to the external radiant heating.

Results

The experimental results will be analyzed and the models will be applied. We would like to assess the accuracy of the models, and their utility for deriving property data for materials tested in the Cone Calorimeter. Properties derived from the literature or by direct measurements are given below:

$\rho = 1190$ kg/m^3 $\qquad$ measured

$$k = 2.49 \times 10^{-7} T + 1.18 \times 10^{-4} \text{ kW/m·K} \qquad [8]$$

$$c = 2.374 \times 10^{-3} T + 1.1 \text{ J/g·K} \qquad [8]$$

$$\alpha = 8.81 \times 10^{-8} \text{ m}^2/\text{s} \qquad [8]$$

Ignition

Figure 6 shows the data for ignition time as a function of external radiant heat flux. For our data, the lines correspond to the application of Eq. (13) with the properties evaluated at a mean temperature with respect to T_{vap}. It appears that better agreement is achieved for a decreasing ignition temperature as the external flux decreases. This is consistent with the data of Figure 5.

Figure 12 shows the same data along with the black PMMA data of Mikkola and Wichman [15] taken in the Cone Calorimeter. Fitting the data below 40 kW/m^2 to a straight line corresponding to the theory (Eq. (13)) gives an intercept of approximately 4 kW/m^2 for the critical heat flux. Solving Eq. (14) for T_{ig} with T_o = 22 C, h_c = 10 W/m^2 K, and ε = 0.95 gives T_{ig} = 180 C. This is lower than we would like to accept, but we will admit it and will proceed to assess its overall effect. Based on the slope of the line, we can also estimate the thermal inertia as follows:

From Eq. (13),

$$\frac{1}{t_{ig}^{2}} = \left[\frac{\varepsilon}{\sqrt{\frac{2}{3} k \rho c \, (T_{ig} - T_o)}}\right] \dot{q}''_{ext} - \left[\frac{h_c (T_{ig} - T_o) + \varepsilon \sigma T_{ig}^4}{\sqrt{\frac{2}{3} k \rho c \, (T_{ig} - T_o)}}\right]. \qquad (31)$$

Using the slope of the fit line in Figure 12,

$$\left[\frac{\varepsilon}{\sqrt{\frac{2}{3} k \rho c \, (T_{ig} - T_o)}}\right] = 0.005053.$$

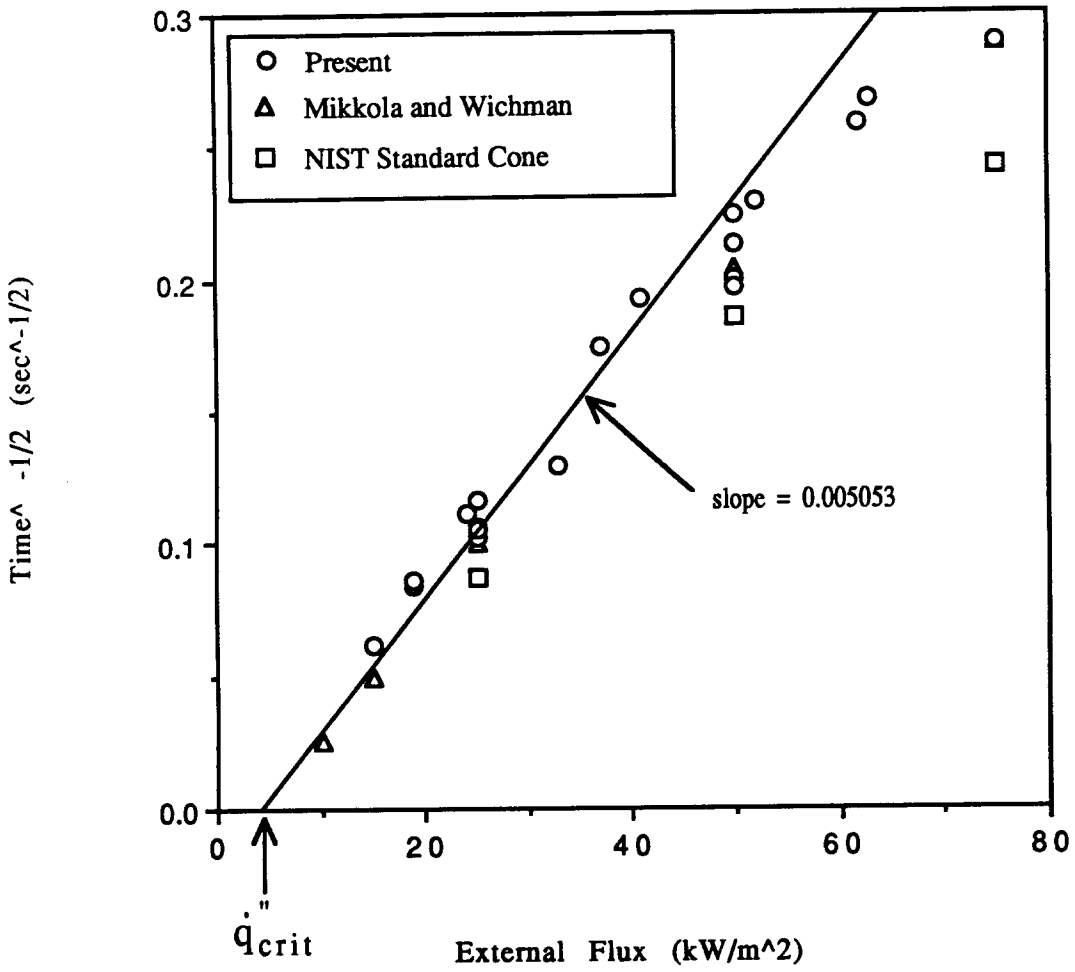

Figure 12. Ignition data for black PMMA

Solving for the thermal inertia,

$$k \rho c = 2.12 \frac{kJ^2}{m^4 \cdot s \cdot K^2} .$$

Since $\rho = 1190$ kg/m^3 and assuming $\alpha = 8.81 \times 10^{-8}$, a constant that can be independantly determined, we can find,

$$k = 0.432 \times 10^{-3} \frac{kW}{m \cdot K}$$

and $$c = 4.12 \frac{kJ}{kg \cdot K} .$$

This gives a prescription for determining k and c provided α is known. The determination of α is still needed, but for most solids, it varies slightly with temperature, and does not vary greatly for non-metals.

Burning Rate

Since PMMA approximates a vaporizing solid, we consider the application of Eq. (28) to the steady state data. The results are plotted in Figure 13 against the external radiant heat flux. The data from our apparatus and the NIST Cone Calorimeter are consistent for the black PMMA. However, the results of Tewarson and Pion [22] are markedly different for clear PMMA because they used a different type of PMMA (Rohm & Hass) compared to ours (Polycast). If the flame heat flux is constant, then,

$$\dot{m}'' L = \dot{q}''_{ext} + \dot{q}''_{fl} - \varepsilon \sigma T_v^4 \qquad (32a)$$

$$\dot{m}'' = \left(\frac{1}{L}\right)\dot{q}''_{ext} + \frac{\left(\dot{q}''_{fl} - \varepsilon\,\sigma\,T_v^4\right)}{L} \qquad (32b)$$

From Figure 13,

$$\left(\frac{1}{L}\right) = 0.361\,\frac{g}{kJ}$$

or $$L = 2.77\,\frac{kJ}{g},$$

and

$$\frac{\dot{q}''_{fl} - \varepsilon\,\sigma\,T_v^4}{L} = 10.0\,\frac{g}{m^2 \cdot s}.$$

For an average vaporization temperature, T_v, of 643 K based on the measured surface temperatures of black PMMA at ignition, and ε taken as 0.95, the steady state average flame flux may be determined using the above equation.

$$\dot{q}''_{fl} \approx 37\,\frac{kW}{m^2}.$$

The heat of gasification corresponding to the Tewarson PMMA is 1.67 kJ/g. An examination of data from radiant heated PMMA in nitrogen are also shown in Figure 13. These correspond to Vovelle et al. [12], Jackson [23] for clear PMMA and Agrawal and Atreya [11] for white PMMA. Their L values are 2.2, 1.96 and 2.73 kJ/g in corresponding order. The wide disparity between the clear and pigmented PMMA samples must indicate a real difference due to composition. This is similar to the variations found by Kashiwagi and Omori for ignition properties [14].

Figure 14 shows the incident flame plus external heat flux to the PMMA surface plotted against the external heat flux. This was done two ways: (1) by sensor measurement, and (2) by calculation from the steady mass loss rate data and assuming L = 2.77 kJ/g. From Eqns. (18) and

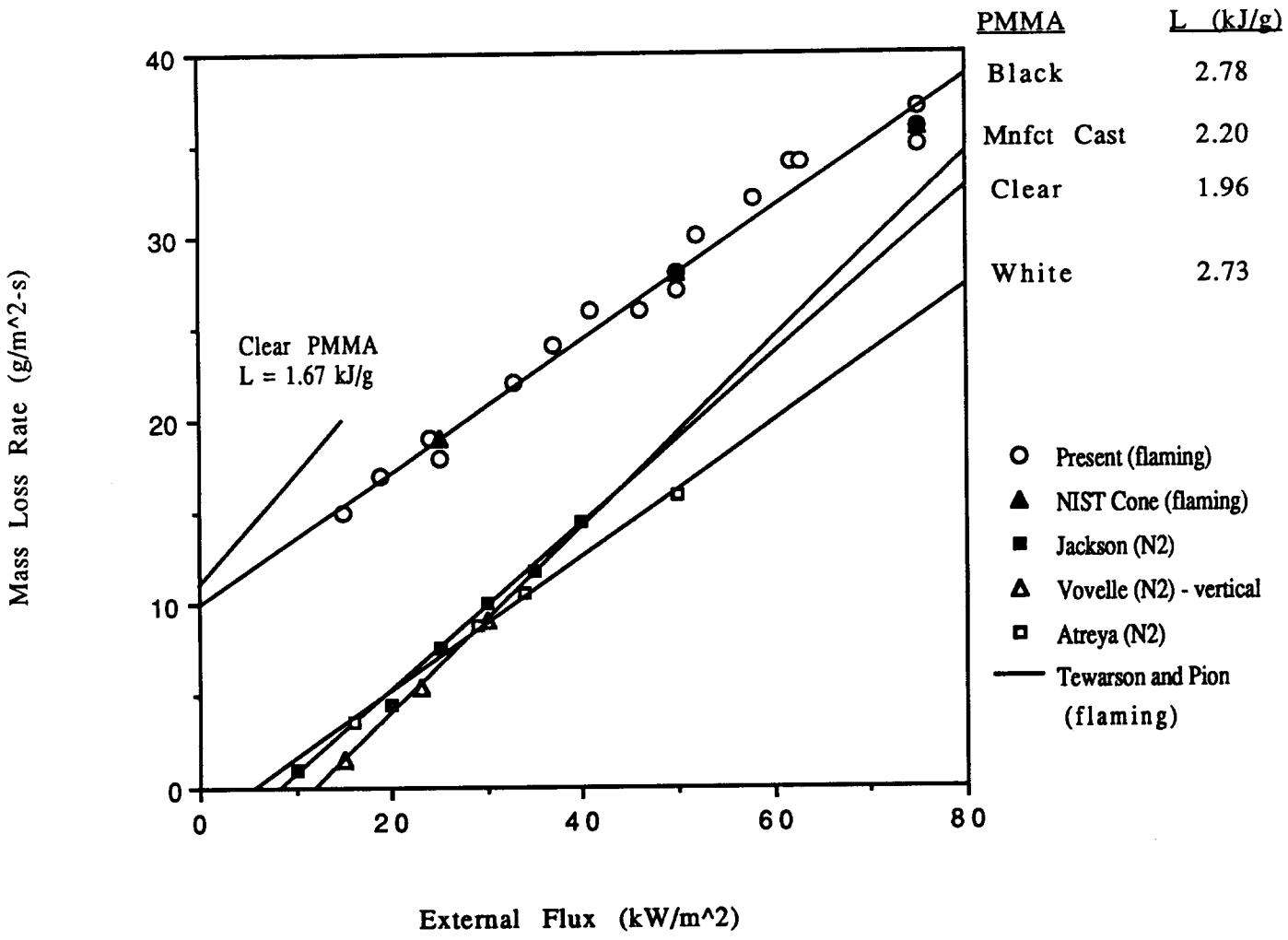

Figure 13. Steady state mass loss rate as a function of external heat flux for flaming and non-flaming PMMA

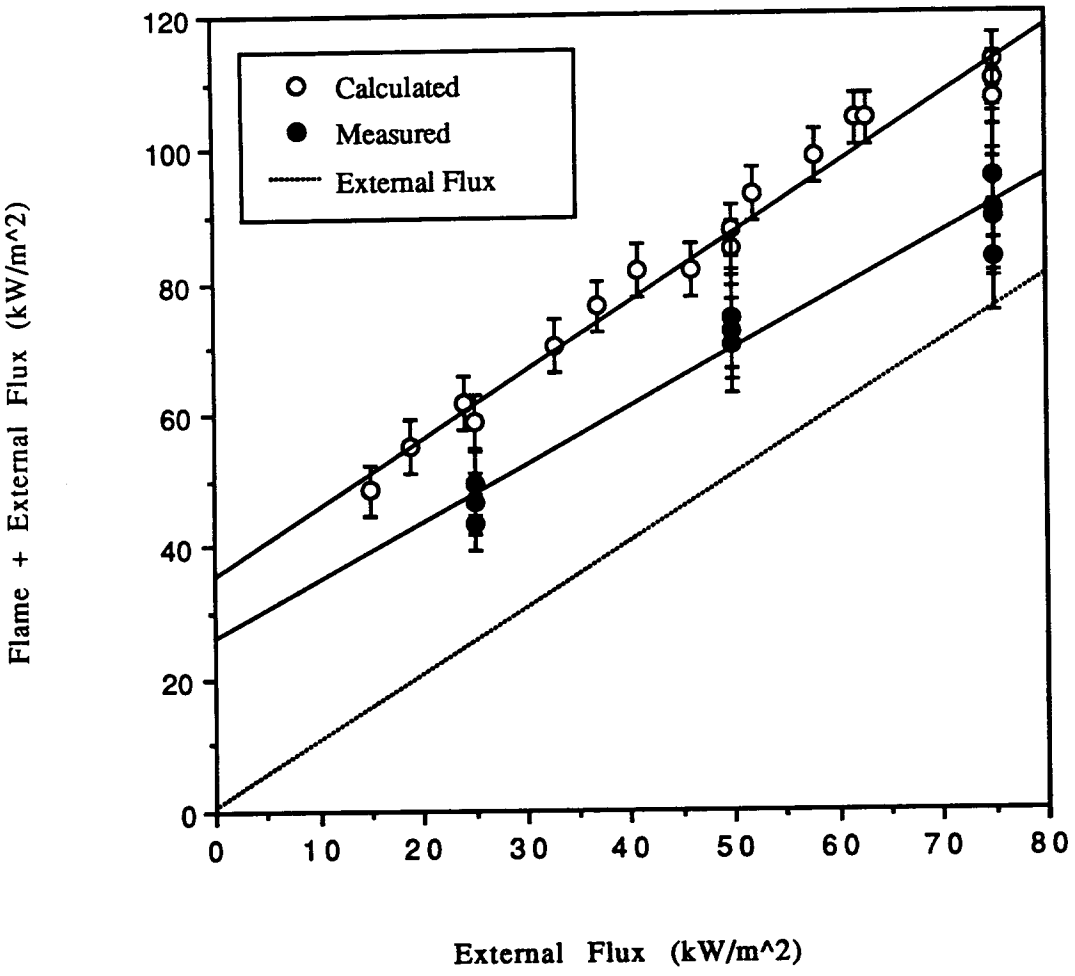

Figure 14. Calculated and measured flame plus external heat flux as a function of external heat flux for black PMMA

(21) applied to the sensor at the water temperature, T_w, the net heat flux to the sensor is,

$$\dot{q}''_{sens} = \dot{q}''_{fl,r} + \dot{q}''_{ext} + h_c \left(\frac{\xi}{e^{\xi} - 1} \right) (T_{fl} - T_w) - \sigma T_w^4 \qquad (33)$$

or,

$$\dot{q}''_{sens} = \dot{q}''_{fl,r} + \dot{q}''_{ext} + h_c \left(\frac{\xi}{e^{\xi} - 1} \right) ((T_{fl} - T_v) + (T_v - T_w)) - \sigma T_w^4 . \qquad (34)$$

The flame and external flux to the PMMA surface measured by the sensor is,

$$\dot{q}''_{fl} + \dot{q}''_{ext} = \dot{q}''_{sens} - h_c \left(\frac{\xi}{e^{\xi} - 1} \right) (T_v - T_w) + \sigma T_w^4 . \qquad (35)$$

This "corrected" sensor flux gives the PMMA value at the center of the sample. Our best data with indicated variability is plotted as shown in Figure 14. The calculated values come from applying Eq. (28) with L = 2.77 kJ/g and T_v corresponding to the measured steady mass loss rate. This gives the average flame plus external heat flux to the PMMA surface. It is higher than the sensor value either because the center has a lower flux than the calculated average flux, or because the sensor has a systematic error. The calculated results yield a constant value for the average flame heat flux of approximately 37 kW/m^2.

Based on this result of the average flame heat flux, Figures 15, 16, 17 show a comparison of calculated mass loss rates compared to data for 25, 50, 75 kW/m^2. The mass loss rates are calculated using Eqns. (23), (25), and the derived properties:

$T_{ig} = T_v = 180\ °C$

$k = 0.432 \times 10^{-3} \frac{kW}{m \cdot K}$

$\rho = 1190 \frac{kg}{m^3}$

$c = 4.12 \frac{kJ}{kg \cdot K}$

$L = 2.77 \frac{kJ}{g}$

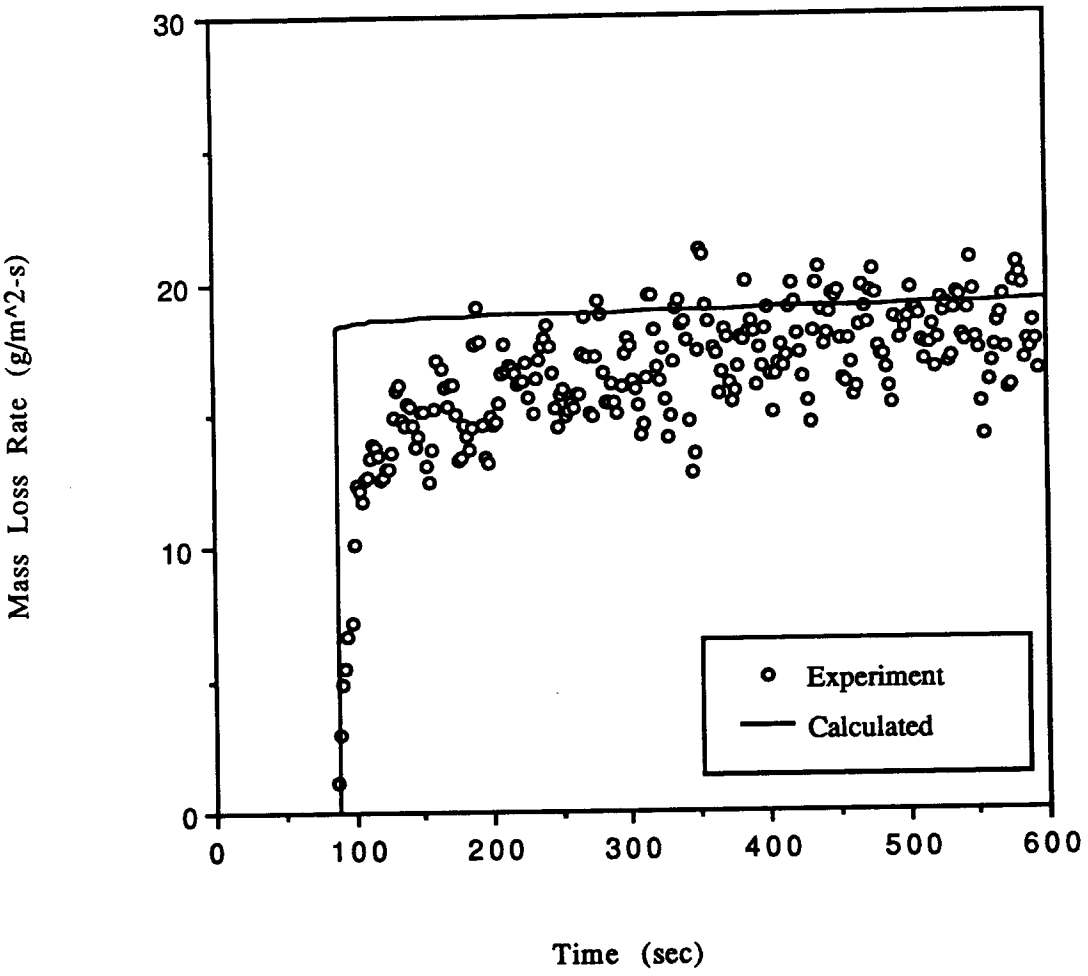

Figure 15. Calculated transient mass loss rates of black PMMA with a 25 kW/m^2 external heat flux

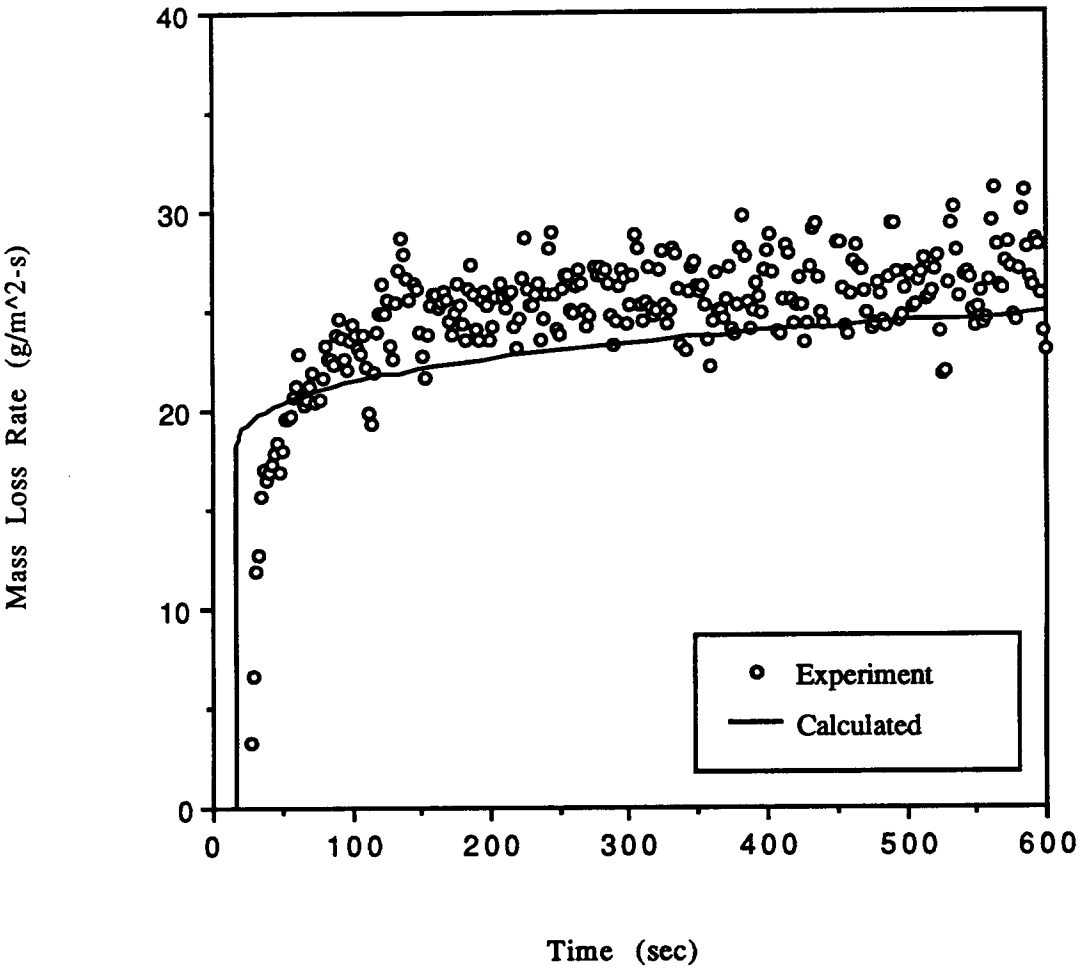

Figure 16. Calculated transient mass loss rates of black PMMA with a 50 kW/m^2 external heat flux

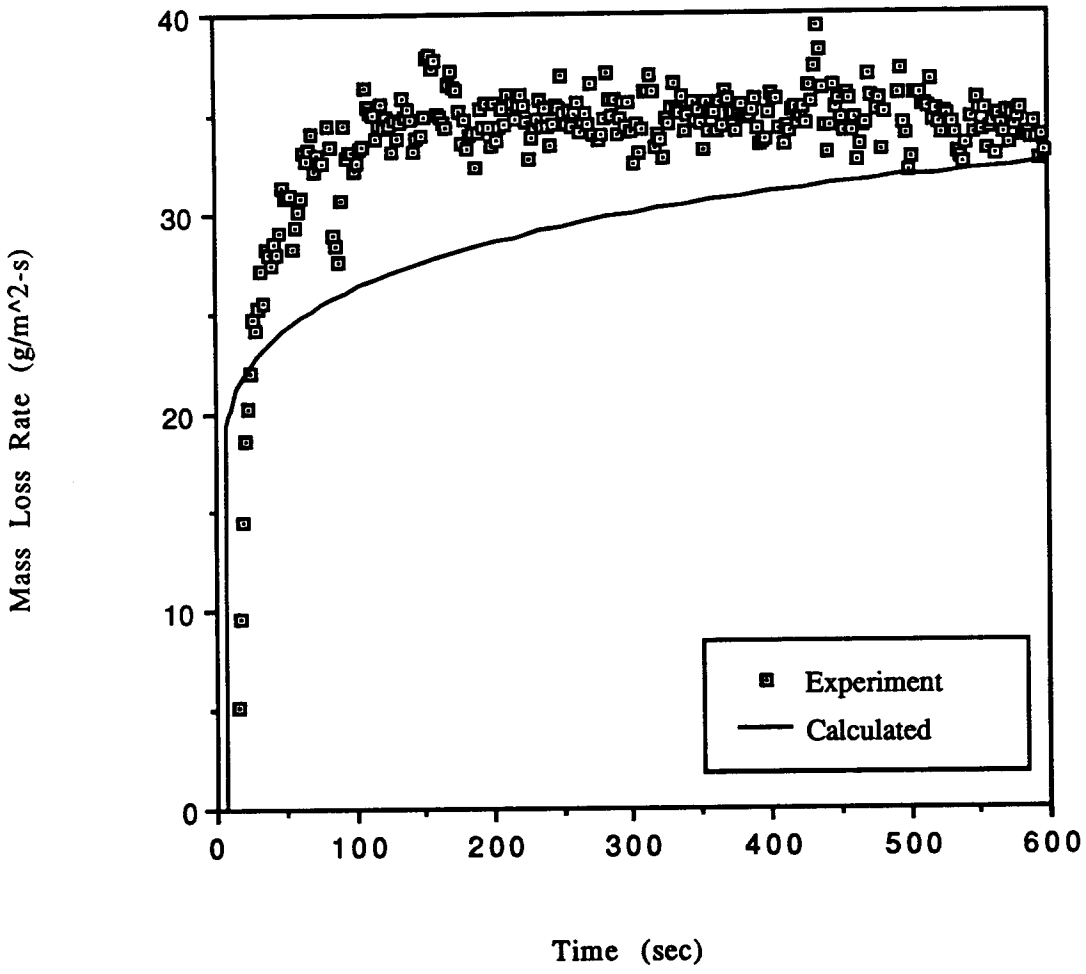

Figure 17. Calculated transient mass loss rates of black PMMA with a 75 kW/m^2 external heat flux

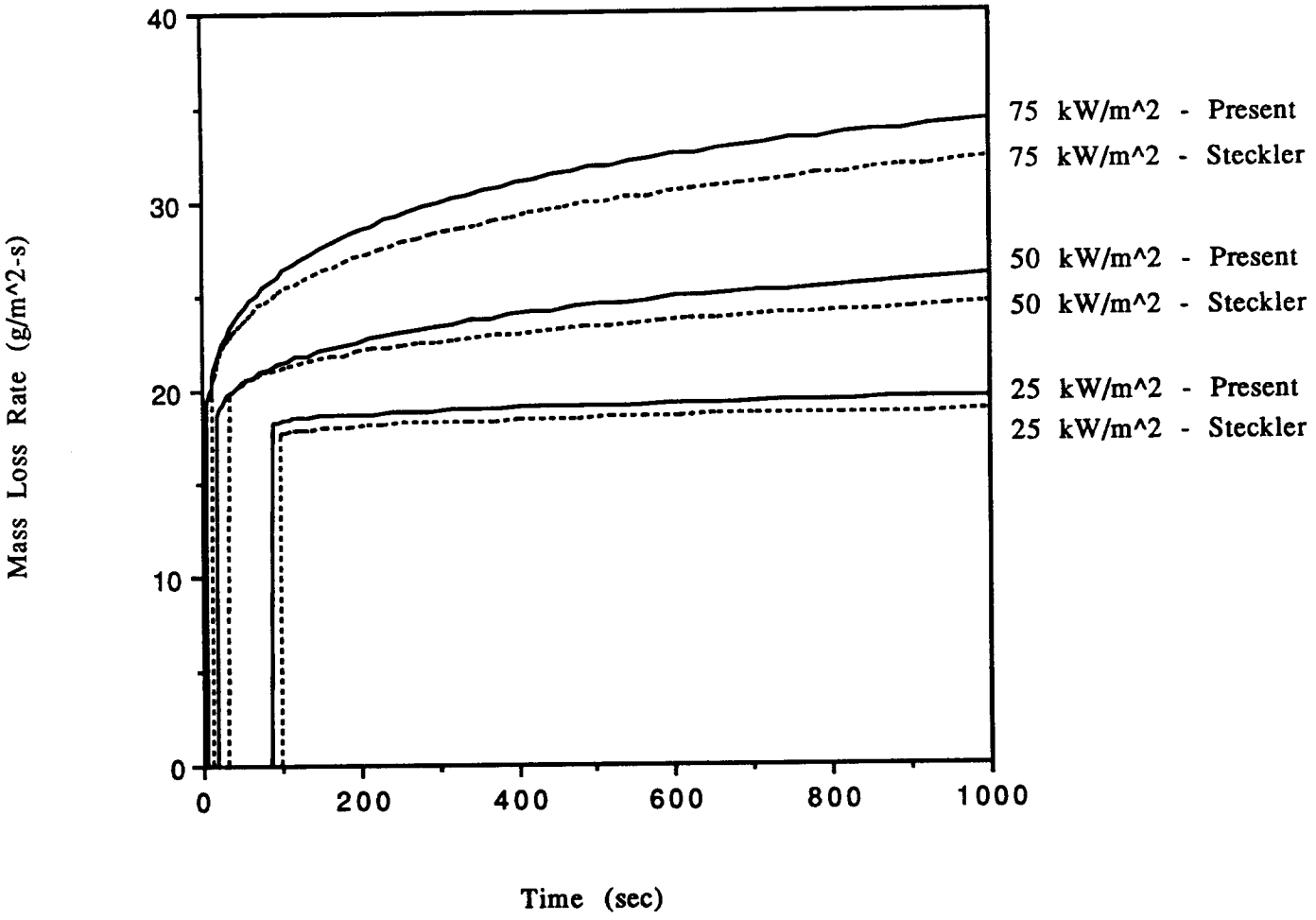

Figure 18. Calculated transient mass loss rates of black PMMA using calculated and literature material property values

The predictions are at worst 20 percent different from the measured transient burning rate. Figure 18 shows the variations in the calculation if the more directly measured (literature) values of T_v, T_{ig}, k and c are used to calculate the mass loss rate, i.e.,

$$T_{ig} = 275 - 360\ ^\circ C \qquad T_v = 365 - 385\ ^\circ C$$

$$k = 0.235 \times 10^{-3}\ \frac{kW}{m \cdot K} \qquad c = 4.12\ \frac{kJ}{kg \cdot K}$$

Conclusions

A modeling prescription has been developed which can use Cone Calorimeter data to derive useful properties needed to predict ignition and transient burning rates for thermoplastic-like materials. The level of accuracy has been demonstrated for PMMA. The low critical flux of PMMA may have given poorer results for the thermal inertia and ignition temperature than would be expected for materials with higher critical fluxes. This is because the ignition model is more accurate at higher fluxes. However, the simplicity of the ignition model is advantageous, and can be used with greater accuracy at higher heat fluxes to infer the critical flux for ignition without direct measurement.

The flame heat flux for samples in the Cone Calorimeter appears to be constant for a given material due to the flame configuration. For black PMMA, this is approximately 37 kW/m^2.

It appears that all PMMA's are not alike, and pigmented samples may have higher heat of gasification values than clear samples. The black Polycast PMMA used in our experiments yielded different results from the Rohm & Hass PMMA used by Tewarson [22] and Jackson [23]. Likewise, the cast PMMA used by Vovelle [12] yielded different results than the Polycast PMMA. This could be due to molecular structure of the sample, as well as the pigmentation.

A test of this testing prescription should be performed by evaluating several different thermoplastic samples.

The heat flux measurement in the flame had many problems due to deposition of the vaporized PMMA. These have not been totally resolved, and appear to be associated with the nature of the phenomena and not necessarily the sensor. A higher temperature sensor may prove better.

Acknowledgement

The authors wish to express their appreciation to Dr. Kashiwagi and Dr. Ohlemiller for their technical support. Further, we would like to thank Mr. E. Braun for his help with the data acquisition system and programming assistance. Brian Rhodes would personally like to thank Mr. R. Shields and Mr. K. Steckler for their assistance in obtaining equipment.

REFERENCES

1. Standard Test Method for Heat and Visible Smoke Release Rates for Materials and Products Using Oxygen Depletion, (ASTM E 1354), American Society for Testing and Materials, Philadelphia, PA.

2. Wickstrom, U. and Goransson, U., "Prediction of Heat Release Rates of Surface Materials in Large-Scale Fire Tests Based on Cone Calorimeter Results", ASTM Journal of Testing and Evaluation, Vol. 15, No. 6, 1987.

3. Karlsson, B. "Modeling Fire Growth on Combustible Lining Materials in Enclosures", Report TVBB-1009, Lund University, Department of Fire Safety Engineering, Lund, Sweden, 1992.

4. Quintiere, J. G., "A Simulation Model for Fire Growth on Materials Subject to a Room-Corner Test", Fire Safety Journal, Vol. 18, 1992.

5. Quintiere, J. G., Haynes, G., and Rhodes, B. T., "Applications of a Model to Predict Flame Spread over Interior Finish Materials in a Compartment", International Conference for the Promotion of Advanced Fire Resistant Aircraft Interior Materials, FAA Technical Center, Atlantic City, NJ, March, 1993.

6. Mitler, H. E., "Algorithm for the Mass-Loss Rate of a Burning Wall", Fire Safety Science Proceedings, Second Internation Symposium, June 13-17, 1988, Tokyo, Japan, Hemisphere Pub. Corp., NY, ed. T. Wakamatsu, 1989.

7. Chen, Y., Delichatsios, M. A. and Motevalli, V., "Materials Pyrolysis Properties, Part I: An Integral Model for One-Dimensional Transient Pyrolysis of Charring and Non-Charring Materials", Combustion Science and Technology, Vol. 88, pp. 309-328, 1993.

8. Steckler, K. D., Kashiwagi, T., Baum, H. R., and Kanemaru, K., "Analytical Model for Transient Gasification of Non-Charring Thermoplastic Materials", Fire Safety Science Proceedings of Third (International) Symposium, pp. 895-904, G. Cox and B. Landford, eds., Elsevier Applied Science, London, 1991.

9. "A Semi-Quantitative Model for the Burning of Solid Materials", National Institute of Standards and Technology, NIST-4840, June, 1992.

10. Quintiere, J. G. and Iqbal, N., "A Burning Rate Model for Materials", accepted by Fire and Materials, July, 1993.

11. Agrawal, S. and Atreya, A., "Wind-Aided Flame Spread over an Unsteady Vaporizing Solid", 24th Symposium (International) on Combustion, The Combustion Institute, Pittsburgh, PA, 1992.

12. Vovelle, C., Delfau, J.L., Reuillon, M., Bransier, J. and Laraqui, N., "Experimental and Numerical Study of the Thermal Degradation of PMMA", Combustion Science and Technology, Vol. 53, pp. 187-201, 1987.

13. Thompson, H. E. and Drysdale, D. D., "Effect of Sample Orientation on the Piloted Ignition of PMMA", pp. 35-42, INTERFLAM, 1990.

14. Kashiwa, T. and Omori, A., "Effects of Thermal Stability and Melt Viscosity of Thermoplastics on Piloted Ignition", 22nd Symposium (International) on Combustion, The Combustion Institue, Pittsburgh, PA, 1988.

15. Mikkola, E. and Wichman, I., "On the Thermal Ignition of Combustible Materials", Fire and Materials, Vol. 14, 1989.

16. Abu-Zaid, M. and Atreya, A., "Effect of Water on Piloted Ignition of Cellulosic Materials", National Institute of Standards and Technology, NIST-GCR-89-561, February, 1989.

17. Janssens, M., "Fundamental Thermophysical Characteristics of Wood and their Role in Enclosure Fire Growth", Doctor of Philosophy Disertation, University of Gent, Belgium, September, 1991.

18. Orloff, L. and deRis, J., "Froude Modeling of Pool Fires", 19th Symposium (International) on Combustion, pp. 885-895, The Combustion Institute, Pittsburgh, PA, 1982.

19. Howell, J. and Siegel, R., Thermal Radiation Heat Transfer, 2nd Edition, Hemisphere Publishing Corporation, New York, 1981.

20. DeRis, J., "Fire Radiation - A Review", 17th Symposium (International) on Combustion, The Combustion Institute, Pittsburgh, PA, 1978.

21. Brosmer, M. A. and Tien, C. L., "Radiative Energy Blockage in Large Pool Fires", Combustion Science and Technology, Vol. 51, no. 1-3, pp. 21-37, Gordon and Breach Science Pub., New York, 1987.

22. Tewarson, A. and Pion, R. F., "Flammability of Plastics - I. Burning Intensity", Combustion and Flame, The Combustion Institute, 1976.

23. Jackson, J. L., "Direct Measurement of Heat of Gasification for Polymethylmethacrylate", National Institute of Standards and Technology, NISTIR 88-3809, September, 1986.

NIST-114
(REV. 6-93)
ADMAN 4.09

U.S. DEPARTMENT OF COMMERCE
NATIONAL INSTITUTE OF STANDARDS AND TECHNOLOGY

MANUSCRIPT REVIEW AND APPROVAL

(ERB USE ONLY)
ERB CONTROL NUMBER | DIVISION
PUBLICATION REPORT NUMBER: NIST-GCR-94-647 | CATEGORY CODE
PUBLICATION DATE: June 1994 | NUMBER PRINTED PAGES

INSTRUCTIONS: ATTACH ORIGINAL OF THIS FORM TO ONE (1) COPY OF MANUSCRIPT AND SEND TO THE SECRETARY, APPROPRIATE EDITORIAL REVIEW BOARD

TITLE AND SUBTITLE (CITE IN FULL)

Fire Growth Models for Materials

CONTRACT OR GRANT NUMBER: 60NANB2D1266

TYPE OF REPORT AND/OR PERIOD COVERED: Final Report June 1992 - December 1993

AUTHOR(S) (LAST NAME, FIRST INITIAL, SECOND INITIAL)
James Quintiere and Brian Rhodes
University of Maryland
Department of Fire Protection Engineering
College Park, MD 20742

PERFORMING ORGANIZATION (CHECK (X) ONE BOX)
[X] NIST/GAITHERSBURG
[ ] NIST/BOULDER
[ ] JILA/BOULDER

LABORATORY AND DIVISION NAMES (FIRST NIST AUTHOR ONLY)

SPONSORING ORGANIZATION NAME AND COMPLETE ADDRESS (STREET, CITY, STATE, ZIP)
U.S. Department of Commerce
National Institute of Standards and Technology
Gaithersburg, MD 20899

PROPOSED FOR NIST PUBLICATION
[ ] JOURNAL OF RESEARCH (NIST JRES)
[ ] J. PHYS. & CHEM. REF. DATA (JPCRD)
[ ] HANDBOOK (NIST HB)
[ ] SPECIAL PUBLICATION (NIST SP)
[ ] TECHNICAL NOTE (NIST TN)
[ ] MONOGRAPH (NIST MN)
[ ] NATL. STD. REF. DATA SERIES (NIST NSRDS)
[ ] FEDERAL INF. PROCESS. STDS. (NIST FIPS)
[ ] LIST OF PUBLICATIONS (NIST LP)
[ ] NIST INTERAGENCY/INTERNAL REPORT (NISTIR)
[ ] LETTER CIRCULAR
[ ] BUILDING SCIENCE SERIES
[ ] PRODUCT STANDARDS
[X] OTHER NIST-GCR-

PROPOSED FOR NON-NIST PUBLICATION (CITE FULLY) [ ] U.S. [ ] FOREIGN

PUBLISHING MEDIUM
[ ] PAPER
[ ] CD-ROM
[ ] DISKETTE (SPECIFY)
[ ] OTHER (SPECIFY)

SUPPLEMENTARY NOTES

ABSTRACT (A 2000-CHARACTER OR LESS FACTUAL SUMMARY OF MOST SIGNIFICANT INFORMATION. IF DOCUMENT INCLUDES A SIGNIFICANT BIBLIOGRAPHY OR LITERATURE SURVEY, CITE IT HERE. SPELL OUT ACRONYMS ON FIRST REFERENCE.) (CONTINUE ON SEPARATE PAGE, IF NECESSARY.)

Ignition and burning rate data have been developed for thick (25 mm.) black Polycast PMMA in a Cone Calorimeter heating assembly. The objective was to establish a testing protocol that would lead to the prediction of ignition and burning rate from Cone data. This has been done for a thermoplastic like PMMA. For black PMMA we measured ignition temperatures of 250 to 350 C and vaporization temperatures of approximately 325 to 380 C over irradiance levels of 15 to 60kW/m^2. The incident flame heat flux, for irradiation levels of 0 to 75 kW/m^2, was found to be approximately 37 kW/m^2 for black PMMA. Its constancy has been shown due to the geometry of the Cone flame. Also, this flame can be shown to be nearly transparent for Cone irradiance (greater than 90 percent). The heat of gasification of the black PMMA used was found to be approximately 2.8 kJ/g: higher than other values reported for PMMA. This is believed to be due to differences in molecular structure or pigmentation effects and the types of PMMA tested. A burning rate model was demonstrated to yield good accuracy (greater than 80 percent) in comparison to measured transient values.

KEY WORDS (MAXIMUM OF 9; 28 CHARACTERS AND SPACES EACH; SEPARATE WITH SEMICOLONS; ALPHABETIC ORDER; CAPITALIZE ONLY PROPER NAMES)
burning rate; cone calorimeters; fire models; heat flux; ignition; pigments; polymethylmethacrylate

AVAILABILITY
[X] UNLIMITED
[ ] FOR OFFICIAL DISTRIBUTION - DO NOT RELEASE TO NTIS
[ ] ORDER FROM SUPERINTENDENT OF DOCUMENTS, U.S. GPO, WASHINGTON, DC 20402
[X] ORDER FROM NTIS, SPRINGFIELD, VA 22161

NOTE TO AUTHOR(S): IF YOU DO NOT WISH THIS MANUSCRIPT ANNOUNCED BEFORE PUBLICATION, PLEASE CHECK HERE. [X]

WORDPERFECT